



This is a postprint version of the following published document:

A.M. Martos, J-Y. Sanchez, A. Várez, B. Levenfeld.  
*Electrochemical and structural characterization of sulfonated polysulfone.*  
Polymer Testing, 45 (2015), pp. 185–193

© 2015 Elsevier Ltd. All rights reserved.

DOI: [10.1016/j.polymertesting.2015.06.004](https://doi.org/10.1016/j.polymertesting.2015.06.004)

---

Material properties

# Electrochemical and structural characterization of sulfonated polysulfone

A.M. Martos <sup>a</sup>, J-Y. Sanchez <sup>a, b</sup>, A. Várez <sup>a</sup>, B. Levenfeld <sup>a, \*</sup>

<sup>a</sup> Department of Materials Science and Engineering and Chemical Engineering, University Carlos III of Madrid, 28911 Leganés, Madrid, Spain

<sup>b</sup> LEPMI UMR 5279 CNRS-Grenoble-INP-UdS-UJF, Bât. PHELMMA, BP.75 Fr., 38402 St. Martin d'Hères Cedex, France

---

## A B S T R A C T

We describe the synthesis, as well as the electrochemical and structural characterization, of sulfonated polysulfone intended for use in PEM fuel cells. Starting from a commercial polysulfone, we assessed the performance of these prepared ionomers using synthesis protocols compatible with industrial production. The efficiency of the trimethylsilyl chlorosulfonate and chlorosulfonic acid reagents in the sulfonation process was confirmed by <sup>1</sup>H NMR, FTIR, elemental analysis, chemical titration and thermal analysis (DSC and TGA). Chlorosulfonic acid was the most effective sulfonation reagent. However, based on SEC MALLS, this reagent induced degradation of the backbone that is detrimental to the thermo-mechanical stability and lifespan of the membranes. The electrical characterization of the membranes was undertaken using impedance spectroscopy in contact with different HCl aqueous solutions at various temperatures. The activation energies, which ranged from 8.2 to 11 kJ/mol, were in agreement with the prevailing proton vehicular mechanism.

---

### Keywords:

Sulfonated polysulfone  
Chlorosulfonic acid  
TMSCS  
Impedance spectroscopy  
PEMFC

## 1. Introduction

Fuel cells, which are the most efficient electrochemical energy conversion sources, are perfectly compatible with other renewable energy sources (i.e., solar and wind energy). The proton exchange membrane fuel cell (PEMFC) has attracted much interest because it is capable of producing high power densities at low temperatures [1]. In addition, its modularity allows for its use as an energy source in various applications from portable electronics to electric cars and stationary applications. Currently, perfluorosulfonated polymer electrolytes, such as Nafion<sup>®</sup> from Dupont or Aquivion<sup>®</sup> from Solvay, are the most widely used electrolytes in PEMFCs due to their high proton conductivity, mechanical properties up to 80 °C and chemical and electrochemical stability. However, this type of membrane also exhibits some drawbacks, which are primarily high cost, low stability at high temperatures, low conductivity at low humidity or high temperature and high methanol crossover in direct methanol fuel cells (DMFCs) [2]. Therefore, extensive studies have been focused on developing alternatives to these perfluorosulfonated membranes [3]. In particular, different polymers

that adopt the sulfonated aromatic hydrocarbon structure have been tested, including poly(arylene ether sulfone)s [4], poly(ether ether ketone)s [5], poly(sulfide sulfone)s [6], polyimides [7], polyphosphazenes [8] and polybenzimidazoles [9].

Among these polymers, polysulfone (PSU) has attracted considerable interest due to its excellent thermomechanical stability, moderate cost and commercial availability. In addition, PSU exhibits resistance to both hydrolysis and oxidizing agents. The diphenylene sulfone endows the polymer backbone with insensitivity to hydrogenation, thermal stability and oxidative resistance [10]. A comparative electrochemical study (i) of model molecules mimicking the backbone of high performance polymers and (ii) their sulfonated form confirmed that the polysulfone ionomers have a wider electrochemical stability window than that of polyether ether ketone and polyphenylene sulfide ionomers [11]. Therefore, sulfonated polysulfone (SPSU) ionomeric membranes have been extensively studied and tested for fuel cell applications [12,13].

In general, two approaches have been used to introduce sulfonic acid groups to these polymers, including the sulfonation of commercial polymers and the polycondensation of sulfonated monomers [4]. The first approach leads to randomly sulfonated polymers and uses polymers that are fairly cheap with high performance. The second approach provides multiblock ionomers. These ionomers

---

\* Corresponding author.

E-mail address: [bl@ing.uc3m.es](mailto:bl@ing.uc3m.es) (B. Levenfeld).

have alternating hydrophobic blocks, which provide good mechanical strength, and hydrophilic ones which provide protonic conductivity. Although the nanostructure of the multi block ionomers is an asset, industrial scale production is challenging. In addition, as in any step growth polymerization, the chain length will strongly depend on the purity of all of the monomers (i.e., the sulfonated monomers).

Because sulfonation proceeds through an electrophilic substitution, it occurs on the electron rich positions of the aromatic rings (i.e., in the ortho position of the ether functions (electron donating resonance effect of oxygen) of the dioxy 2,2 diphenylpropane moiety). Sulfonation on an electron poor position (i.e., diphenylsulfone rings) must allow for a decrease in the desulfonation of the ionomers and a slight increase in the dissociation of the sulfonic acids. Kerres et al. [14] previously proposed a 3 step reaction that leads to these alternative ionomers. This clever approach led to a wide variety of structured polysulfone ionomers. However, sulfonating polysulfone in this position requires the use of highly concentrated solutions of butyllithium, which makes large scale production of the ionomer questionable. Currently, the easiest and cheapest upscaling process involves electrophilic substitution of commercially available high performance polymers. Sulfonation of bisphenol A based poly(ether sulfone) (PES) by chlorosulfonic acid was first reported by Quentin [15]. Noshay and Robeson demonstrated PSU sulfonation using the sulfur trioxide/triethyl phosphate complex [10]. Then, this complex [16], chlorosulfonic acid [13,17], and trimethylsilyl chlorosulfonate ( $\text{ClSO}_3\text{Si}(\text{CH}_3)_3$ ) [12,18] were studied as sulfonating agents in electrophilic substitution. However, sulfuric acid failed because the polymer was neither swelled nor dissolved in the strong acid solvent [17].

In this study, we compare the sulfonation of PSU using two sulfonating reagents (i.e., the industrial route ( $\text{ClSO}_3\text{H}$ ) compared to the laboratory one ( $\text{ClSO}_3\text{Si}(\text{CH}_3)_3$ ). The degree of sulfonation (DS) was estimated by  $^1\text{H}$  NMR, elemental analysis, ion exchange capacity (IEC) and thermogravimetric analysis. Special attention was paid to the determination of the actual molecular weights that govern the membrane brittleness. Irrespective of the sulfonation protocol, the concentration in the sulfonic groups, which is expressed by the DS, determines the performance (e.g., mechanical and thermal properties, water uptake, IEC and proton conductivities) of sulfonated polysulfones in membrane applications.

Electrochemical impedance spectroscopy (EIS) was used to study the electrical properties of the membranes. The measurements were carried out with the membranes in contact with HCl aqueous solutions at different concentrations. The analysis of the impedance plots using equivalent circuits as models identified the different contributions to the total conductivity. The study of the conductivity at different temperatures allowed us to obtain the activation energy associated with the membrane, as well as determining the primary mechanism involved in the diffusion process.

## 2. Experimental

### 2.1. Materials

Polysulfone ( $M_n = 26,000$  g/mol), chlorosulfonic acid ( $\text{ClSO}_3\text{H}$ , 98%), trimethylsilyl chlorosulfonate ( $\text{ClSO}_3\text{Si}(\text{CH}_3)_3$ , TMSCS, 99%), N,N dimethylacetamide (DMAc), 1,2 dichloroethane (DCE), DMF  $d_7$  and DMSO  $d_6$  were supplied by Sigma–Aldrich (Sant Louis, USA). The solvents were high grade reagents and used as received.

### 2.2. Sulfonation of PSU

First, the sulfonation process was carried out in anhydrous

conditions under  $\text{N}_2$  following the method described by Chao et al. [19]. Therefore, the solution of PSU in DCE was treated with TMSCS or  $\text{ClSO}_3\text{H}$  diluted in DCE. The mixture was maintained under magnetic stirring for 24 h using TMSCS and 4 h using  $\text{ClSO}_3\text{H}$  at room temperature. Once the reaction was complete, the sulfonated polymer (SPSU) was purified until a neutral pH was achieved. Finally, the obtained polymer was dried at room temperature. The PSU:TMSCS molar ratios were 1:1, 1:3 and 1:6, and the PSU: $\text{ClSO}_3\text{H}$  molar ratios were 1:1 and 1:3.

### 2.3. Membrane preparation

The SPSU in the salt form was dissolved in DMAc to prepare a 5 wt % solution under magnetic stirring for 24 h at room temperature. The polymeric solution was cast on a Petri glass dish and dried in an oven using the following thermal cycle: 60 °C for 24 h, 90 °C for 1 h, 120 °C for 1 h and 165 °C for 1 h. Finally, the membranes were immersed in water to eliminate possible traces of the solvent, followed by drying at room temperature. The thickness of the obtained membranes was in the range of 50–100  $\mu\text{m}$ .

### 2.4. Characterization and measurements

#### 2.4.1. $^1\text{H}$ NMR analysis

The liquid  $^1\text{H}$  NMR spectra of polymers were recorded on a Bruker Avance DPX 300 MHz spectrometer. DMF  $d_7$  was used as the solvent for PSU, and DMSO  $d_6$  was used as the solvent for SPSU. In addition, tetramethylsilane was used as the internal reference.

#### 2.4.2. FT IR analysis

The Fourier transform infrared spectra of the polymers were recorded on an FTIR spectrometer Perkin–Elmer Spectrum GX in the 4000–400  $\text{cm}^{-1}$  range using 16 scans at a resolution of 4  $\text{cm}^{-1}$ .

#### 2.4.3. Size exclusion chromatography

Size exclusion chromatography (SEC) was performed on a modular system equipped with an HPLC pump 515 Series, PolarGel M D column, refractive index (RI) detector 2000 and DAWN light scattering (LS) detector. LS and viscosity measurements of the ionomers required the use of a solvent with a specific ionic strength to avoid effects from dilution on ionic polymer dissociation, which modifies the chain solvent interaction. Therefore, the samples ( $\text{Na}^+$  form) were dissolved in an eluent (i.e., 0.1 M solution of  $\text{NaNO}_3$  in DMF) at a flow rate of 1.0 ml/min. The  $dn/dc$  (specific refractive index increment) values were calculated from the measurements assuming 100% mass recovery ( $dn/dc = 0.13\text{--}0.17$  ml/g). The molecular weights were determined from the LS signal using the Astra 6 software (Wyatt Tech, USA). The fit of the molecular weight/elution volume dependence in the complete range of the RI signal was used to estimate the distribution of the lower molecular weight species that cannot be detected by the LS detector but are visible in the RI signal [20].

#### 2.4.4. Elemental analysis

Elemental analysis (EA) of the polymers based on the sulfur to carbon ratio was performed with a manual FlashEA elemental analyser. C, H, N and S were converted to  $\text{CO}_2$ ,  $\text{H}_2\text{O}$  and  $\text{N}_2$  at 900 °C in a column containing an oxidizing agent. These molecules were separated in a GC column containing molecular sieves and detected by a thermal conductivity detector (TCD). The percentages of C, H, N and S were determined after elaboration of the respective calibration curves for different standards.

#### 2.4.5. Ion exchange capacity

The IEC values of the membranes were determined by classical

titration. The membrane samples in their acidic form (after exchange in 1 M HCl solution for at least 24 h) were immersed in a 2 M NaCl solution for 24 h to release the protons. The resulting solutions were titrated using 0.01 M NaOH with phenolphthalein as an indicator.

The IEC values were calculated from Equation (1):

$$IEC_{ex}(\text{equiv/g}) = \frac{V_{NaOH} \times [NaOH]}{W_{dry}} \quad (1)$$

$V_{NaOH}$  is the volume of NaOH consumed.

$[NaOH]$  is the concentration of NaOH.

$W_{dry}$  is the weight of the membrane in the dry state.

#### 2.4.6. Thermal analysis

Thermal characterization of the polymers was performed by thermogravimetric analysis (TGA) and differential scanning calorimetry (DSC). The TGA experiments were carried out with a Perkin Elmer Pyris TGA1. The analyses were performed under nitrogen between 50 and 850 °C at a heating rate of 10 °C/min. The DSC measurements were performed under nitrogen with a Perkin Elmer Diamond calorimeter. The samples were heated from 50 to 300 °C at a heating rate of 10 °C/min, and the temperature was maintained for 5 min at both temperatures followed by cooling at 20 °C/min. Then, the samples were heated once more under the same conditions. The midpoint of the enthalpy increment in the transition region of the second heating was used to determine the  $T_g$ .

#### 2.4.7. Mechanical measurements

The mechanical properties of the wet membranes were measured at room temperature on a Universal Testing Machine (Shimadzu model Ag 1) with a 1 kN load cell at a strain rate of 0.5 mm min<sup>-1</sup>. The size of the samples was 25 mm × 5 mm. Prior to mechanical testing, the samples were immersed in water for 3 h.

#### 2.4.8. Water uptake (WU)

The WU values of the different membranes were determined at room temperature. The samples were immersed for 72 h in deionized water. After quickly wiping off the excess water from the surface, all of the samples were weighed. After drying at 60 °C for 24 h, the samples were weighed again to determine the mass in the dry state.

The WU was calculated using Equation (2):

$$WU(\%) = \frac{W_{wet} - W_{dry}}{W_{dry}} \times 100 \quad (2)$$

where  $W_{wet}$  and  $W_{dry}$  are the masses of the membranes in the wet and dry state, respectively.

#### 2.4.9. Impedance spectroscopy

The proton conductivity of the membranes was determined using an AC impedance technique in a test cell consisting of two half cells [21] in which the membrane was sandwiched between two o rings. A conventional electrochemical setup consisting of four electrodes was used for these measurements. The four electrodes consisted of two saturated Ag/AgCl electrodes as reference electrodes and two graphite electrodes as secondary electrodes. The impedance spectra of the membranes were recorded in the 10<sup>-1</sup> and 10<sup>6</sup> Hz frequency range by applying a voltage of 10 mV. In these experiments, an impedance/gain phase analyser (Solartron 1260) and an electrochemical interface (Solartron 1287) were used.

Prior to each measurement, the membranes were immersed in 10<sup>-3</sup> M HCl for 24 h, and six different HCl solutions (10<sup>-3</sup> ≤ c ≤ 10<sup>-1</sup> M) were tested. First, the measurements were conducted at room temperature. The resistance value associated with the membrane was determined from the intercept with the real axis of the high frequency impedance values in the Nyquist plots. The membrane conductivities ( $\sigma$  in S/cm) were calculated from the membrane resistance (R) using the following equation:

$$\sigma = \frac{l}{R \times A} \quad (3)$$

where  $l$ ,  $R$  and  $A$  are the membrane thickness in cm, the resistance in ohms and the cross sectional area of the membrane in cm<sup>2</sup>, respectively.

Measurements at different temperatures (30–80 °C) were performed under the same conditions using a climatic chamber KMF 115 (Binder GmbH). A dwell time of 15 min was employed prior to making each measurement.

The activation energy ( $E_a$  in kJ/mol) was calculated using Equation (4).

$$\ln \sigma - \ln A = \frac{E_a}{RT} \quad (4)$$

where  $\sigma$ ,  $A$ ,  $R$  and  $T$  are the proton conductivity in S/cm, the pre exponential factor, the ideal gas constant in J/mol K and the temperature in K, respectively.

## 3. Results and discussion

### 3.1. Study of the sulfonation

In a previous study, Genova Dimitrova et al. [12] reported the disadvantages of the ClSO<sub>3</sub>H reagent. Sulfonation modifies the hydrophilicity of the polymer (SO<sub>3</sub>H groups), which rapidly precipitates in DCE, and the reaction continues in a heterogeneous mode. The trapping of HCl, which is a by product in the precipitate, leads to chain breaking that affect the mechanical strength of the SPSU. In contrast, sulfonation with TMSCS, leads to the ester form of the ionomer, which remains soluble in DCE. However, despite the ester form of ClSO<sub>3</sub>H (i.e., ClSO<sub>3</sub>Si(CH<sub>3</sub>)<sub>3</sub>) being less aggressive, chain breaking has been reported when the reaction was performed under a moderate flux of inert gas [18]. Following this work, we studied the sulfonation using both reagents. In both cases, successful sulfonation of polysulfone was confirmed by <sup>1</sup>H NMR and FTIR analyses. In addition, the possible degradation of the polymer by the sulfonation was studied by SEC MALLS. Finally, the influence of sulfonic groups on the glass transition temperature was studied by DSC.

#### 3.1.1. <sup>1</sup>H NMR analysis

The sulfonation reaction was successfully confirmed using <sup>1</sup>H NMR spectroscopy. The PSU spectra are shown in Fig. 1 a. The proton resonance at ~7.3 ppm was assigned to the proton labelled "2". The SPSU spectra with TMSCS (left) and ClSO<sub>3</sub>H (right) are shown in Fig. 1 b. In this case, the peak associated with the proton adjacent to the new sulfonic acid groups appears at ~7.7 ppm. The presence of the –SO<sub>3</sub>H group results in a significant downfield shift of hydrogen 2 at 0.4 ppm compared to 2 and 2'' in the bis phenol A ring [18].

#### 3.1.2. FT IR analysis

The sulfonation of polysulfone was also confirmed using FTIR spectroscopy (data not shown). In the frequency range of

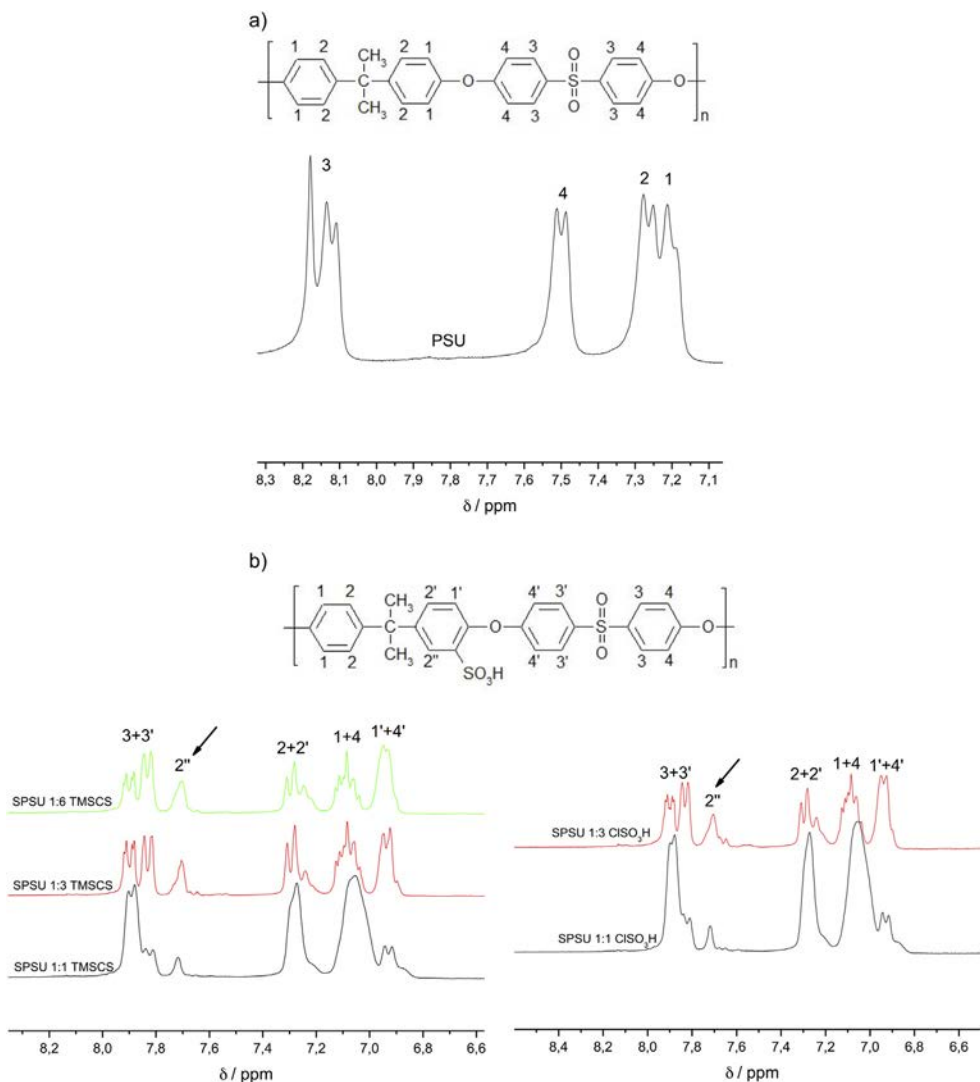


Fig. 1. NMR spectra of a) PSU and b) SPSU membranes.

1050–1000  $\text{cm}^{-1}$ , two characteristic peaks were observed [22]. In particular, the band located at 1014  $\text{cm}^{-1}$  was due to the symmetric stretching vibration of the diphenylether unit, and the peak at 1028  $\text{cm}^{-1}$  was assigned to the symmetric stretching vibration of the sulfonated group. The different spectra were normalized because the peak at 1014  $\text{cm}^{-1}$  was independent of the DS. As expected, the symmetric peak at 1028  $\text{cm}^{-1}$  increased with the DS (data not shown).

These results indicated the presence of sulfonic groups in the polymer backbone after the sulfonation reaction.

### 3.1.3. Differential scanning calorimetry

The  $T_g$  values of the different SPSU membranes were determined using DSC. The presence of sulfonic groups in the poly sulfone backbone modifies the glass transition temperature ( $T_g$ ). The  $T_g$  values obtained for SPSU 1:1  $\text{ClSO}_3\text{H}$ , SPSU 1:3 TMSCS and SPSU 1:6 TMSCS were 207, 199 and 221  $^\circ\text{C}$ , respectively. In some cases (1:1 TMSCS), the visualization of the  $T_g$  was unclear. The introduction of sulfonic groups in a ring on the bis phenol A unit supplies a more rigid structure. The sulfonic groups induced (i) interchain hydrogen bonding between the acidic moieties and (ii) bulkiness. The bulkiness hinders the internal rotation of high molecular chain segments, increasing the  $T_g$  of SPSU [22,23].

### 3.1.4. Size exclusion chromatography

The sulfonation process degrades the main chain of polymers [12]. To assess this degradation, we performed molecular weight analyses of PSU and different SPSU using SEC MALLS. The average molecular weights ( $M_n$ ) and polydispersity indices (PDI) are shown in Table 1. The  $M_n$  decreased sharply with the sulfonation using  $\text{ClSO}_3\text{H}$  as the reagent. The TMSCS reagent also resulted in a decrease in the  $M_n$  with similar PDI but to a lesser degree. This result may be due to the super acidity of  $\text{ClSO}_3\text{H}$ , which is a very strong sulfonating agent. The heterogeneous nature of the reaction leads to intimate trapping of HCl in the precipitated polymer, which favours chain breaking. It is important to note that unidimensional polymers obtained by polycondensation have much lower  $M_n$  than

Table 1  
 $M_n$  and PDI of polysulfone and SPSU determined by SEC-MALLS.

Polymer	GPC SEC-MALLS	
	$M_n$ (g/mol)	PDI
PSU	26620	2.2
SPSU 1:1 $\text{ClSO}_3\text{H}$	13810	1.7
SPSU 1:1 TMSCS	18450	1.8
SPSU 1:3 TMSCS	18350	1.8

polymers made by polyaddition (i.e., free radical, anionic or cationic polymerization). Therefore, chain breaking, which strongly decreases the entanglements, has a higher impact on the mechanical performance of polycondensates. However, the reaction mixture remains perfectly homogeneous when a mild sulfonating reagent (TMSCS) was used [18].

### 3.2. Degree of sulfonation

The DS was calculated using four different techniques (i.e.,  $^1\text{H}$  NMR, EA, IEC and TGA). Table 2 shows the results obtained.

#### 3.2.1. $^1\text{H}$ NMR analysis

The polysulfone can be sulfonated up to two sulfonic groups per monomer repeat unit. As shown in Fig. 1 b, the substitution occurs on the diphenyl ether unit (i.e., first in position 1' leading to a monosubstituted product ( $\text{DS} \leq 1$ ) and then in position 1 resulting in a disubstituted product ( $\text{DS} > 1$ )). Because sulfonation is an electrophilic reaction, it depends on the substituent present on the ring. Therefore, electron donating substituents favour the reaction, and electron withdrawing ones impede it.

The spectra of SPSU (Fig. 1 b) indicate that sulfonation leads to several new peaks (i.e., 1', 2', 2'', 3', and 4'), the intensity of which grows with the DS. This parameter was quantified using the R ratio. This value is related to the peak integrals or aromatic protons according to Kopf's formula [18]. To evaluate the sulfonic group content, we calculated the R ratio according to the following equation:

$$R = \frac{I(1, 1', 2, 2', 4, 4)}{I(2'', 3, 3')} = \frac{12 \cdot 2\text{DS}_{\text{NMR}}}{4 + 2\text{DS}_{\text{NMR}}} \quad (5)$$

where I corresponds to the peak integrals and  $\text{DS}_{\text{NMR}}$  is the degree of sulfonation.

#### 3.2.2. Elemental analysis

The DS of the polymers was indirectly determined by CHNS elemental analysis. In the polysulfone, the monomeric unit has a molecular weight of 442 g/mol, and the  $\text{SO}_3\text{H}$  unit has a molecular weight of 80 g/mol. The percentages of C, H, N and S obtained and the degree of sulfonation are shown in Table 2. DS was determined using equation (6):

$$\text{DS}_{\text{EA}} = \frac{\left(\frac{\%S}{100}\right) \times M_{\text{polymer}}}{M_S \left(\frac{\%S}{100}\right) \times M_{\text{SO}_3\text{H}}} \cdot 32 \quad (6)$$

$M_{\text{polymer}}$  442 g/mol.  $M_{\text{polymer}}$  is the molecular weight of the polymer repeat unit.

$M_{\text{SO}_3\text{H}}$  80 g/mol.  $M_{\text{SO}_3\text{H}}$  is the molecular weight of the  $-\text{SO}_3\text{H}$  group.

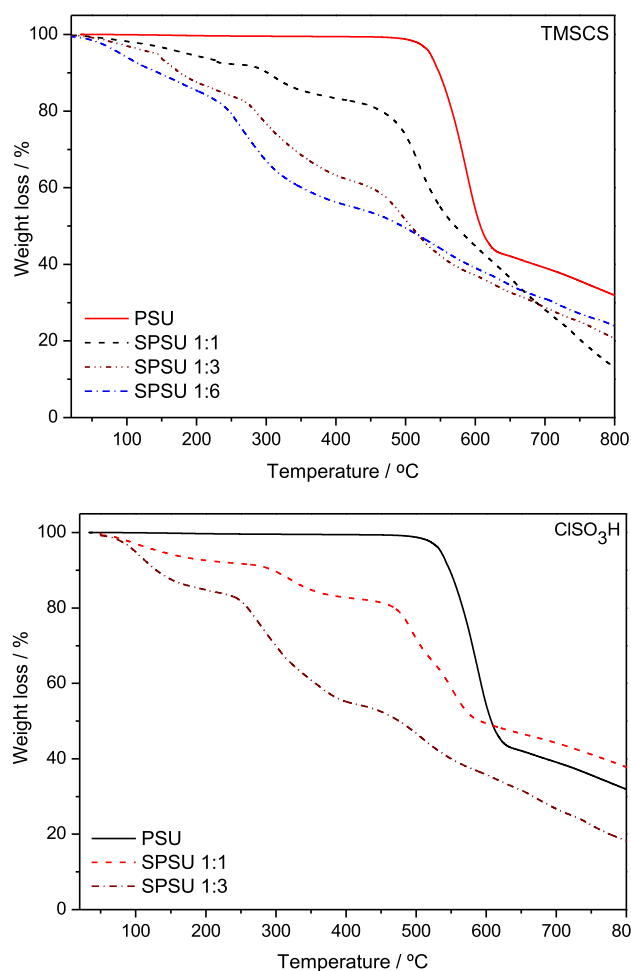


Fig. 2. TGA curves for PSU and SPSU.

$M_S$  32 g/mol.  $M_S$  is the atomic weight of S. The %S value was provided by the instrument

#### 3.2.3. Ion exchange capacity

The DS of the studied membranes was calculated from the experimental IEC values using the following equation:

$$\text{DS}_{\text{IEC}} = \frac{\text{IEC}/1000}{\left(1 - \left(\frac{\text{IEC}/1000}{80}\right)\right) \times (1/442)} \quad (7)$$

The IEC values and calculated DS are listed in Table 2. Despite the low reaction time, the IEC value for SPSU 1:1  $\text{ClSO}_3\text{H}$  was higher than that observed for SPSU 1:1 TMSCS. This result indicated that

Table 2

DS of sulfonated polysulfone determined using four different techniques:  $^1\text{H}$  NMR, EA, TGA and IEC.

Polymer	$^1\text{H}$ -NMR	Elemental Analysis				IEC	TGA		DS <sub>TGA</sub>	
	DS <sub>NMR</sub>	%C	%H	%N	%S		DS <sub>EA</sub>	IEC <sub>ex</sub>		DS <sub>IEC</sub>
PSU	-	72.67	5.03	0.15	7.05	-	-	-	-	
SPSU 1:1 $\text{ClSO}_3\text{H}$	0.28	56.90	4.25	0	10.42	0.59	0.73	0.34	9.1	0.55
SPSU 1:3 $\text{ClSO}_3\text{H}$	0.86	44.66	4.01	0	13.33	1.26	-	-	27.6	2.10
SPSU 1:1 TMSCS	0.37	59.01	4.5	0.07	9.29	0.37	0.53	0.24	8.7	0.53
SPSU 1:3 TMSCS	0.77	48.66	4.27	0	12.18	0.98	1.15	0.53	21.0	1.46
SPSU 1:6 TMSCS	0.96	42.85	4.61	0	12.88	1.15	-	-	25.0	1.84



$\text{ClSO}_3\text{H}$  was the most reactive sulfonation reagent.

### 3.2.4. Thermal analysis

The thermal stability of PSU and SPSU was studied by TGA. The decomposition curves of PSU and SPSU with both sulfonating reagents are shown in Fig. 2. As the SPSU:TMSCS/ $\text{ClSO}_3\text{H}$  molar ratio increased, the thermal stability of the polymer decreased. However, the results indicated that the thermal stability of SPSU is adequate within the conceivable temperature range for PEMFC application.

TGA curves of SPSU exhibited a three step degradation pattern compared to the single step degradation of PSU. The weight loss at temperatures ranging from 50 to 200 °C corresponds to the loss of absorbed water, which interacts with the hydrophilic sulfonic groups. The second weight loss between 200 °C and 400 °C was due to the desulfonation process, which involves evolution of  $\text{SO}_2$  and  $\text{SO}$  gases. Finally, the third weight loss above 450 °C is related to main chain polymer decomposition. Similar results were observed for other sulfonated high performance polymers [24]. The second weight loss was used to assess the DS of the modified polymers using equation (8).

$$DS_{TGA} = \frac{M_{\text{polymer}}}{EW} \frac{EW}{M_{\text{SO}_3\text{H}}} \frac{1}{(W_{\text{loss}}/100)/M_{\text{SO}_3\text{H}}} \quad (8)$$

$M_{\text{polymer}}$  is the molecular weight of the repeat unit of the non ionic polymer (442 g/mol).

$M_{\text{SO}_3\text{H}}$  is the molecular weight of the  $-\text{SO}_3\text{H}$  group (80 g/mol).

$W_{\text{loss}}$  is the second weight loss corresponding to the decomposition of the  $-\text{SO}_3\text{H}$  group.

All of the techniques used to determine the DS are in agreement with the increase in the amount of sulfonation reagent. The results are all consistent with each other, demonstrating that  $\text{ClSO}_3\text{H}$  is the most efficient sulfonating reagent in terms of both the reaction rate and reaction yield. The DS inferred from these techniques are compared in Fig. 3. The DS deduced from the TGA was always higher than those obtained using other techniques. The difference between the techniques increased as the DS increased. This gap can be explained by the difficulty in clearly distinguishing between the onset of weight loss due to the loss of sulfonic groups, which corresponds to the decomposition temperature of the polymeric backbone that is most likely catalysed by the released acidic groups. This difficulty results from the shape of the baseline. Iojoiu et al. [18] reported the limitations of EA. Due to the hygroscopic nature of the ionomers, the DS obtained from EA are lower than those inferred from  $^1\text{H}$  NMR spectra. In our case, the main limitation of the EA data may be related to the presence of some impurities (e.g., residual reagent) in the sample, which increased the amount of sulfur. For the DS inferred from the IEC, the error may be due to an incomplete  $\text{Na}^+/\text{H}^+$  exchange related to the possible inaccessibility of some sulfonic acid groups embedded in the bulk of the ionomer. In fact, IEC led to the lowest DS values. In conclusion, the  $^1\text{H}$  NMR spectra provided the highest accuracy and the most realistic values.

### 3.3. Mechanical measurements

The mechanical properties of the wet membranes at room temperature are shown in Table 3.

For the SPSU using TMSCS, the tensile strength and Young's modulus values progressively decreased as the DS increased. This may be due to the hydrophilic character of the sulfonic groups, which allowed water to behave like an external plasticizer. This decrease in the Young modulus has been previously reported and

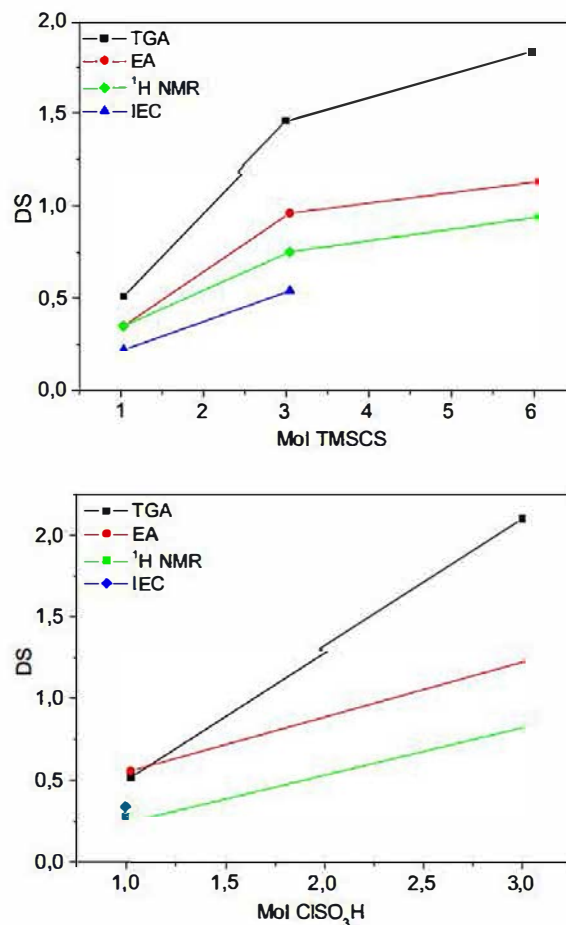


Fig. 3. DS obtained by different techniques ( $^1\text{H}$  NMR, EA, TGA and IEC) for the prepared membranes.

was to an increase in the polymer chain mobility [12].

The tensile strength was slightly lower in the SPSU obtained using  $\text{ClSO}_3\text{H}$ , and the elongation at break and the Young's modulus were slightly higher. Based on the high performance polymeric backbone, all of the SPSU exhibited a much higher tensile strength and Young's modulus than Nafion 117, and a much lower elongation at break.

### 3.4. Impedance spectroscopy

The proton conductivities of the membranes were measured by EIS by immersing the membranes in HCl aqueous solutions with various concentrations ranging from  $10^{-3}$  M–0.1 M. The Nyquist plots of SPSU 1:3 TMSCS as a function of different HCl concentrations are shown in Fig. 4 a. These plots exhibit two semicircles, which change with the HCl concentration. The first semicircle (high frequency arc (HFA)) is related to the membrane capacitance, and the low frequency arc (LFA) is deformed and associated with the diffusion of the electroactive species [25]. In all of the cases, the HFA does not intercept the origin of the plot, indicating the presence of a resistive element in series with the other two processes, which is most likely related to the electrolyte. The Nyquist plots of SPSU 1:1 TMSCS and SPSU 1:1  $\text{ClSO}_3\text{H}$  exhibited a similar behaviour (results not shown).

The equivalent circuit for the different membrane/solution systems is shown in the inset of Fig. 4 a. Two pseudo RC elements are associated in series with a resistive element  $R_1$  (associated with

**Table 3**

Mechanical properties of the SPSU membranes and Nafion 117. The DS of each membrane, which was determined by  $^1\text{H}$  NMR spectroscopy, have been included.

Membrane	DS <sub>NMR</sub>	Tensile strength (MPa)	Elongation at break (%)	Young's modulus (MPa)
Nafion 117 [27]		18	190	153
SPSU 1:1 TMSCS	0.37	32.4	11.49	783
SPSU 1:3 TMSCS	0.77	10.34	11.49	557
SPSU 1:1 ClSO <sub>3</sub> H	0.28	29.15	12.86	1002

electrolyte), which is also in series. The first element (resistance in parallel with a constant phase element (CPE)) is due to the membrane. The second element (a parallel association of resistance and Warburg) is related to the liquid electrolyte solution separating the membrane and the electrodes. The fitting of the experimental data was carried out using non linear fitting software [26]. For the following discussion, we only considered the membrane contribution.

As expected, the conductivity of the membrane increased with the HCl concentration (Fig. 4 b) and was attributed to the concentration dependence of the liquid electrolyte solution embedded in the membrane matrix [21]. The evolution of the real part of the admittance with the frequency for the SPSU 1:3 TMSCS membrane for different HCl concentrations is shown in Fig. 4 c. The real part of the admittance values was basically independent of the frequency; indicating that dc conductivity is maintained over the entire frequency range. This behaviour was also observed for the other membranes (data not shown). This pure impedance resistive (dc conductivity) was also observed in the Bode plot (Fig. 4 d), where the phase angle is close to zero in a very broad frequency range. This result is in agreement with a cationic transference number ( $T^+$ ) that is rigorously equal to 1 for the ionomeric membrane and close to 1 in any aqueous acidic solution. In this case, contact ion pairs (the less acidic arylsulfonic groups) and free ions coexist. However, the non dissociated moieties will be immobile (both anion and  $\text{H}^+$ ) due to the dissociated moieties and, therefore,  $T^+$  is equal to 1.

We also analysed the influence of the DS on the transport properties. The impedance plots of the membranes with different DS values and in contact with a 0.05 M HCl solution are shown in Fig. 5 a. The HFA decreased with the DS, indicating an improvement in the conductivity with the presence of the sulfonic groups. It is important to note that the sample treated with ClSO<sub>3</sub>H exhibited a lower DS with a slightly higher conductivity. This result may be related to the degradation of the polymer backbone. In Fig. 5 b, the evolution of the conductivity and water uptake for different DS values is plotted. At room temperature, the amount of absorbed water increases with DS, in relation with the increased hydrophilicity.

The proton transport in the polymeric membranes is typically described by two mechanisms [27]. i) The first is the "Grotthuss mechanism", which involves the protons hopping across the membrane from one acidic site (sulfonic groups surrounded by water molecules) to the next one through hydrogen bonds. This mechanism exhibits high thermal activation energy due to the formed hydrogen bonds ( $E_a \approx 14\text{--}40 \text{ kJ mol}^{-1}$ ) [28]. (ii) The second mechanism is the "vehicular mechanism", which assumes that the proton diffuses together with the solvent molecules by forming a complex, such as  $\text{H}_3\text{O}^+$  or  $\text{H}_5\text{O}_2^+$ . This mechanism is characterized by  $E_a$  that is lower than those in the Grotthuss mechanism [29].

To analyse the proton transport mechanism in these membranes, we studied the conductivity as a function of temperature. For example, Fig. 6 a shows the evolution of the Nyquist plots with temperature for the SPSU 1:3 TMSCS sample. The HFA was shifted

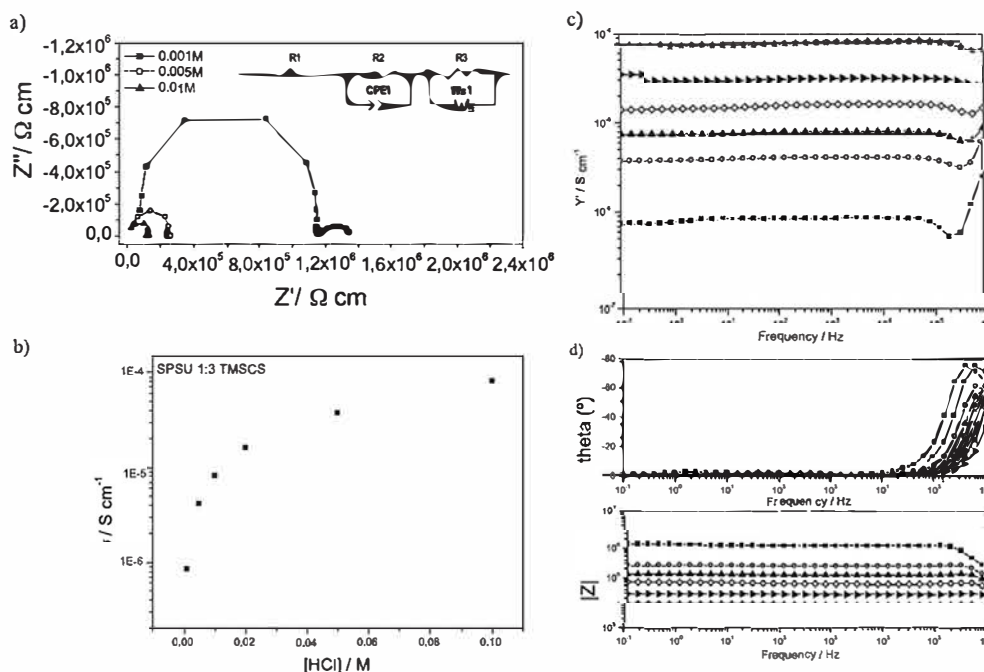


**Fig. 4.** a) Impedance plot at room temperature and equivalent circuit for SPSU 1:3 TMSCS in contact with different HCl concentrations. b) Evolution of the conductivity of the SPSU 1:3 TMSCS membrane as a function of the HCl concentration. c) Admittance plot for the SPSU 1:3 TMSCS membrane at different HCl concentrations. d) Bode diagrams for the SPSU 1:3 TMSCS membrane at different HCl concentrations showing the logarithm of the impedance modulus and phase angle ( $\theta$ ).



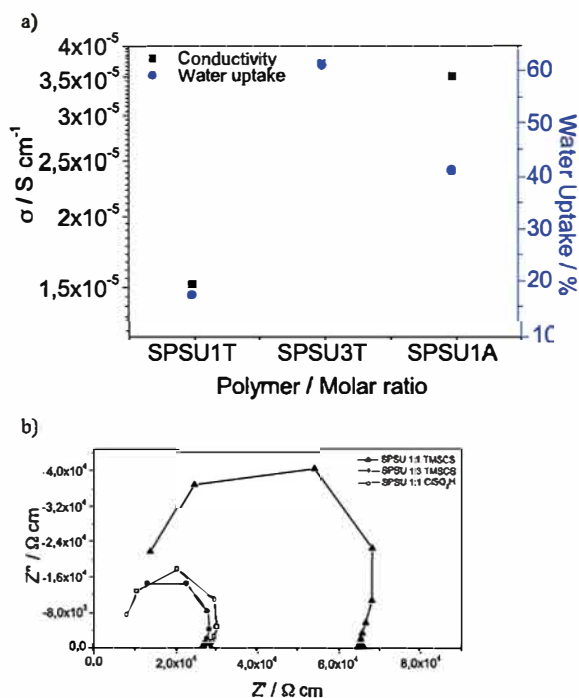


Fig. 5. a) Water uptake and proton conductivity at room temperature for the different membranes. b) Nyquist plot for the different membranes in contact with a 0.05 M HCl solution.

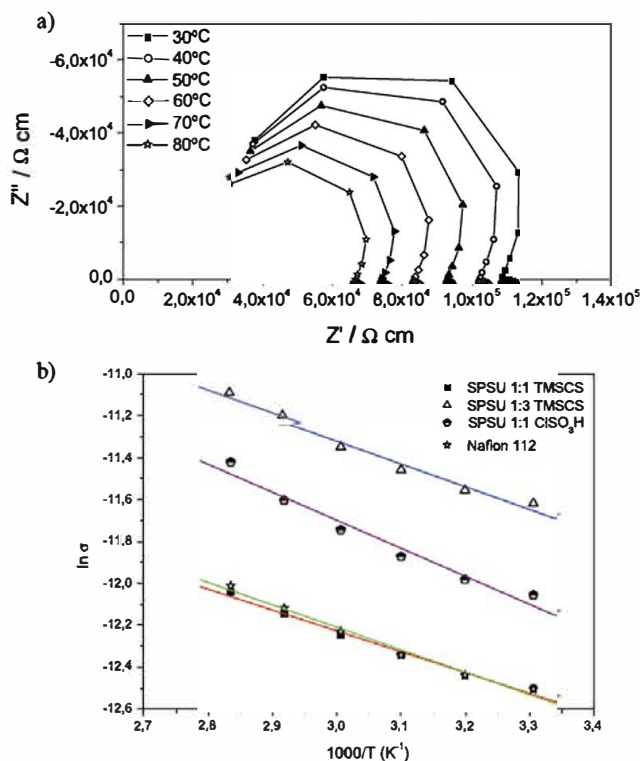


Fig. 6. a) Nyquist plot for the SPSU 1:3 TMSCS membrane ( $[HCl] = 10^{-2} M$ ) at different temperatures. b) Evolution of the proton conductivity as a function of temperature for the prepared membranes. The data were obtained from the Nyquist plot (see the text). The values are compared to that obtained for Nafion 112.

Table 4  
Activation energy for the prepared membranes.

Membrane	Ea (KJ/mol)
Nafion 112	$8.9 \pm 0.5$
SPSU 1:1 TMSCS	$8.2 \pm 0.5$
SPSU 1:3 TMSCS	$9.0 \pm 0.6$
SPSU 1:1 ClSO <sub>3</sub> H	$11 \pm 1$

to lower values as the temperature increased, indicating an increase in the conductivity. The evolution of the real part of the admittance with the frequency for different temperatures was also analysed (data not shown). For each temperature, these values were independent of the frequency, indicating dc conductivity in the entire analysed frequency range. The temperature dependence on the proton conductivity of SPSU 1:3 TMSCS is shown in Fig. 6 b. The conductivity increased with temperature following Arrhenius type behaviour according to equation (4). The Ea for the different membranes are listed in Table 4. These values were not significantly different, and they were similar to the one we obtained for commercial membranes of Nafion 112 and that reported by Qiao et al. for Nafion 117 (12 kJ/mol) [27]. These results indicated that the vehicular model is the main proton transport mechanism in all the membranes and is independent of the sulfonating reagent used to synthesize the ionomers.

#### 4. Conclusions

PSU was successfully sulfonated using two different sulfonating reagents (i.e., TMSCS and ClSO<sub>3</sub>H). A wide range of characterizations was performed to determine the DS, indicating that NMR was the most accurate method. The Mn and PDI of the ionomers confirmed that despite careful experimental conditions, ClSO<sub>3</sub>H produced significant chain breakages, which were much more important than those induced by TMSCS, and consistent with the results reported by Iojoiu et al. [11]. Although ClSO<sub>3</sub>H may appear more suitable for scaling up, we must emphasize that the expensive TMSCS can be easily generated in situ from a mixture of fairly cheap reagents (i.e.,  $(ClSi(CH_3)_3)$  and ClSO<sub>3</sub>H). In addition, the moderate chain breakages using TMSCS could be avoided using a high gas flux to eliminate the HCl formed in the reaction. If this gas flux was an inert gas in research laboratories, it could be advantageously replaced by dry air during industrial production.

Although most of the conductivities of the PEMFC membranes are reported under different relative humidities, we selected a useful and simple electrochemical device to estimate the proton transport in these membranes under wet conditions. Therefore, the Arrhenius type behaviour was observed for all of the elaborated membranes, and the small Ea confirmed proton transport by a predominant vehicular mechanism.

#### Acknowledgements

This study was supported by the Ministry of Science and Innovation with a project MAT2013 46452 C4 3 R and the Regional Program MATERENER3CM S2013/MIT 2753 of the Community of Madrid. J Y Sanchez also wishes to thank "Catedras de Excelencia" of Universidad Carlos III de Madrid for providing a grant. A.M. Martos wishes to thank the mobility grant of Universidad Carlos III de Madrid.

#### References

- [1] S. Kordes, G. Simader, *Fuel for the Fuel Cell Technology Fuel Cells and Their Applications*, Wiley-VCH, 1996.

- [2] V. Di Noto, E. Negro, J.-Y. Sanchez, C. Iojoiu, Structure relaxation interplay of a new nanostructured membrane based on tetraethylammonium trifluoromethanesulfonate ionic liquid and neutralized Nafion 117 for high-temperature fuel cells, *J. Am. Chem. Soc.* 132 (2010) 2183.
- [3] S.J. Peighambaroust, S. Rowshanzamir, M. Amjadi, Review of the proton exchange membranes for fuel cell applications, *Int. J. Hydrogen Energy* 35 (2010) 9349.
- [4] F. Wang, M. Hickner, Y.S. Kim, T.A. Zawodzinski, J.E. McGrath, Direct polymerization of sulfonated poly(arylene ether sulfone) random (statistical) copolymers: candidates for new proton exchange membranes, *J. Membr. Sci.* 197 (2002) 231.
- [5] P. Xing, G.P. Robertson, M.D. Guiver, S.D. Mikhailenko, K. Wang, S. Kaliaguine, Synthesis and characterization of sulfonated poly(ether ether ketone) for proton exchange membranes, *J. Membr. Sci.* 229 (2004) 95.
- [6] M. Schuster, K.D. Kreuer, H.T. Andersen, J. Maier, Sulfonated poly(phenylene sulfone) polymers as hydrolytically and thermooxidatively stable proton conducting ionomers, *Macromolecules* 40 (2007) 598.
- [7] K. Miyatake, H. Zhou, T. Matsuo, H. Uchida, M. Watanabe, Proton conductive polyimide electrolytes containing trifluoromethyl groups: synthesis, properties and DMFC performance, *Macromolecules* 37 (2004) 4961.
- [8] Q. Guo, P.N. Pintauro, H. Tang, S. O'Connor, Sulfonated and crosslinked polyphosphazene-based proton-exchange membranes, *J. Membr. Sci.* 154 (1999) 175.
- [9] J.S. Wainright, J.T. Wang, D. Weng, R.F. Savinell, M. Litt, Acid-doped polybenzimidazoles- a new polymer electrolyte, *J. Electrochem Soc.* 142 (1995) L121.
- [10] A. Noshay, L.M. Robertson, Sulfonated polysulfone, *J. Appl. Polym. Sci.* 20 (1976) 1885.
- [11] C. Iojoiu, M. Maréchal, F. Chabert, J.-Y. Sanchez, Mastering sulfonation of aromatic polysulfones: crucial for membranes for fuel cell application, *Fuel Cells* 5 (2005) 344.
- [12] P. Genova-Dimitrova, B. Baradie, D. Foscallo, C. Poinsignon, J.Y. Sanchez, Ionomeric membranes for proton exchange membrane fuel cell (PEMFC): sulfonated polysulfone associated with phosphoantimonic acid, *J. Membr. Sci.* 185 (2001) 59.
- [13] F. Lufrano, I. Gatto, P. Staiti, V. Antonucci, E. Passalacqua, Sulfonated polysulfone ionomer membranes for fuel cells, *Solid State Ionics* 145 (2001) 47.
- [14] J. Kerres, A. Ullrich, F. Meier, T. Haring, Synthesis and characterization of novel acid-base polymer blends for application in membrane fuel cells, *Solid State Ionics* 125 (1999) 243.
- [15] J.P. Quentin, Sulfonated polyarylethersulfones, United States patent U.S. 3,709,841, 1973 Jan 9.
- [16] J.F. O'Gara, D.J. Williams, W.J. Macknight, F.E. Karasz, Random homogeneous sodium polysulfone ionomers: preparation, characterization and blend studies, *J. Polym. Sci. Part B Polym. Phys.* 25 (1987) 1519.
- [17] J.F. Blanco, Q.T. Nguyen, P. Schaezel, Sulfonation of polysulfones: suitability of the sulfonated materials for asymmetric membrane preparation, *J. Appl. Polym. Sci.* 84 (2002) 2461.
- [18] C. Iojoiu, P. Genova-Dimitrova, M. Marechal, J.-Y. Sanchez, Chemical and physicochemical characterization of ionomers, *Electrochim. Acta* 51 (2006) 4789.
- [19] S.Y. Chao, D.R. Eelsey, Process for preparing sulfonated poly(arylether)resins, United States patent US 4,625,000, 1996 Nov 25.
- [20] H. Kombert, S. Chakraborty, B. Voit, S. Banerjee, Degree of sulfonation and microstructure of post-sulfonated polyethersulfone studied by NMR spectroscopy, *Polymer* 53 (2012) 1624.
- [21] J. Benavente, A. Canas, M.J. Ariza, A.E. Lozano, J. De Abajo, Electrochemical parameters of sulfonated poly-ether ether sulfone/membranes in HCl solutions determined by impedance spectroscopy and membrane potential measurements, *Solid State Ionics* 145 (2001) 53.
- [22] Y. Devrim, S. Erkan, N. Bac, I. Eroglu, Preparation and characterization of sulfonated polysulfone titanium dioxide composite membranes for proton exchange membrane fuel cells, *Int. J. Hydrogen Energy* 34 (2009) 3467.
- [23] R. Pedicini, A. Carbone, A. Sacca, I. Gatto, G. Di Marco, E. Passalacqua, Sulfonated polysulphone membranes for medium temperature in polymer electrolyte fuel cells (PEFC), *Polym. Test.* 27 (2008) 248.
- [24] K.S. Kim, K.H. Lee, K. Cho, C.E. Park, Surface modification of polysulfone ultrafiltration membrane by oxygen plasma treatment, *J. Membr. Sci.* 199 (1-2) (2002) 135.
- [25] M. Herrero, A.M. Martos, A. Várez, J.C. Galván, B. Levenfeld, Synthesis and characterization of polysulfone/layered double hydroxides nanocomposite membranes for fuel cell application, *Int. J. Hydrogen Energy* 39 (2014) 4016.
- [26] Zview for Windows, Impedance/Gain Phase Graphing and Analysis Software, Scribner Associates Inc, Southern Pines, NC, USA, 2012.
- [27] J. Qiao, T. Hamaya, T. Okada, Chemically modified poly(vinyl alcohol)-poly(2-acrylamide-2-methyl-1-propanesulfonic acid) as a novel proton-conducting fuel cell membrane, *Chem. Mater.* 17 (2005) 2413.
- [28] Y. Li, Q.T. Nguyen, P. Schaezel, C. Lixon-Buquet, L. Colasse, V. Ratieville, S. Marais, Proton exchange membranes from sulfonated polyetheretherketone and sulfonated polyethersulfone-cardo blends: conductivity, water sorption and permeation properties, *Electrochim. Acta* 111 (2013) 419.
- [29] P. Colomban, A. Novak, P. Colomban (Eds.), Proton Conductors, Cambridge University Press, Cambridge, England, 1992, pp. 35-55.